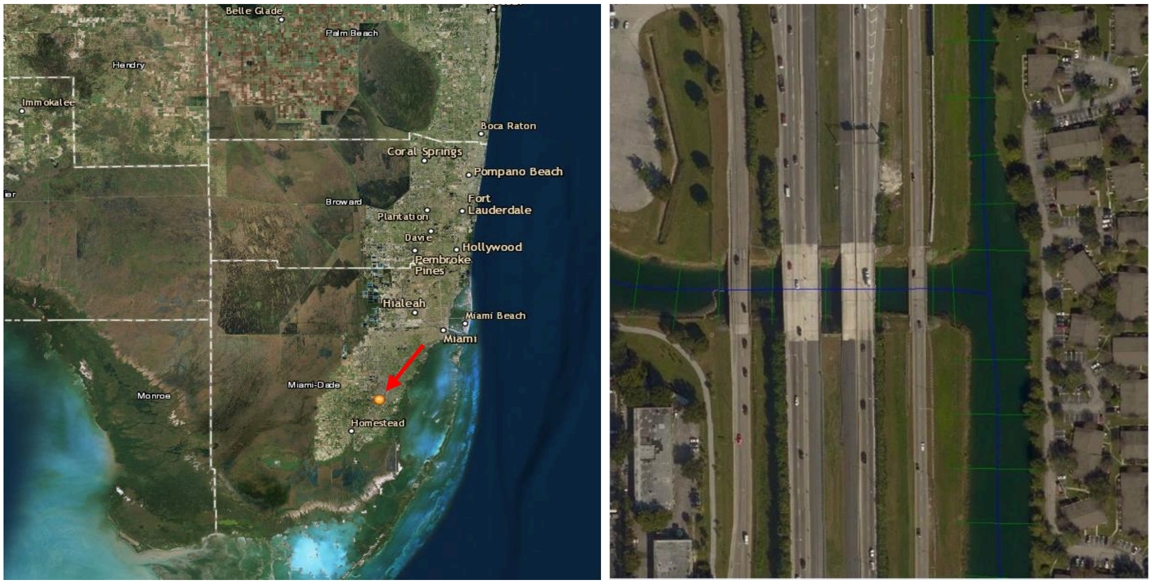

Figure 9. C1N junction location and C1-C1N canal cross-section locations

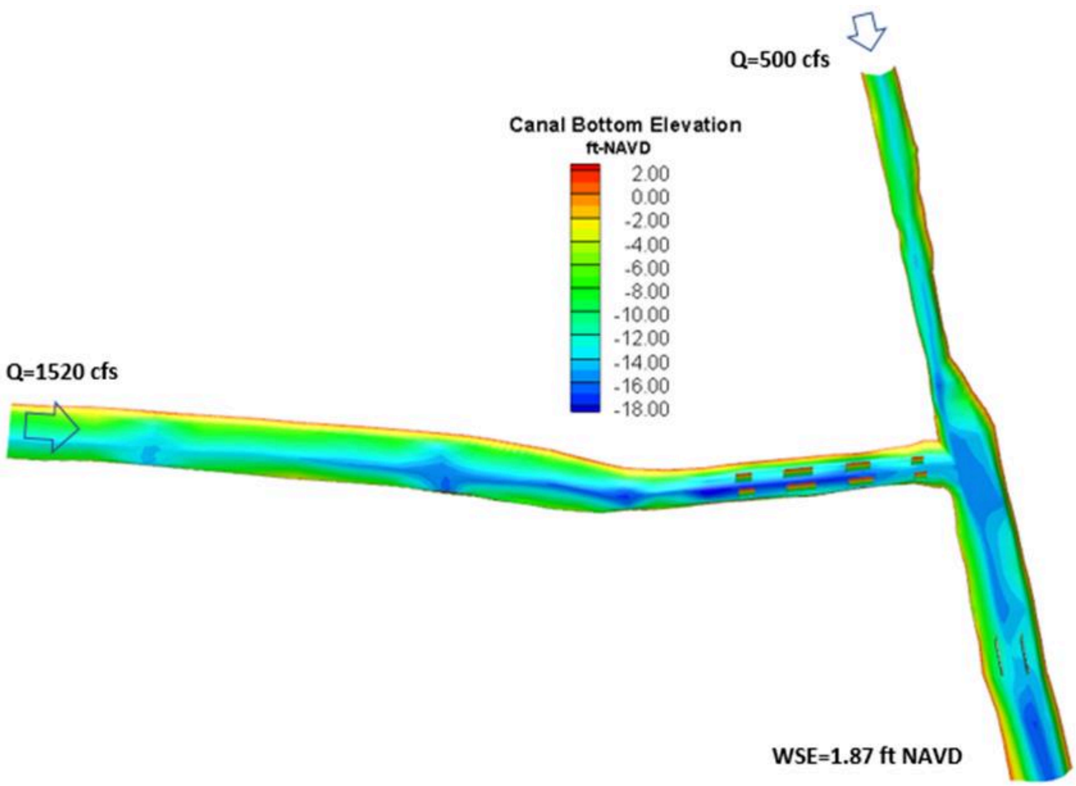

Figure 10. C1N junction canal bathymetric contours

The C1N junction canal bathymetry and simulation domain are shown in Figure 10. The west canal becomes deeper near the junction with canal bottom elevation about -16 ft-NAVD. In the upstream location, the west canal has a bottom elevation of -10 to -12 ft-NAVD. For the north canal, the bottom elevation is about -10 ft-NAVD in the upstream, -14 ft-NAVD near the junction, and -15 ft-NAVD in the downstream.

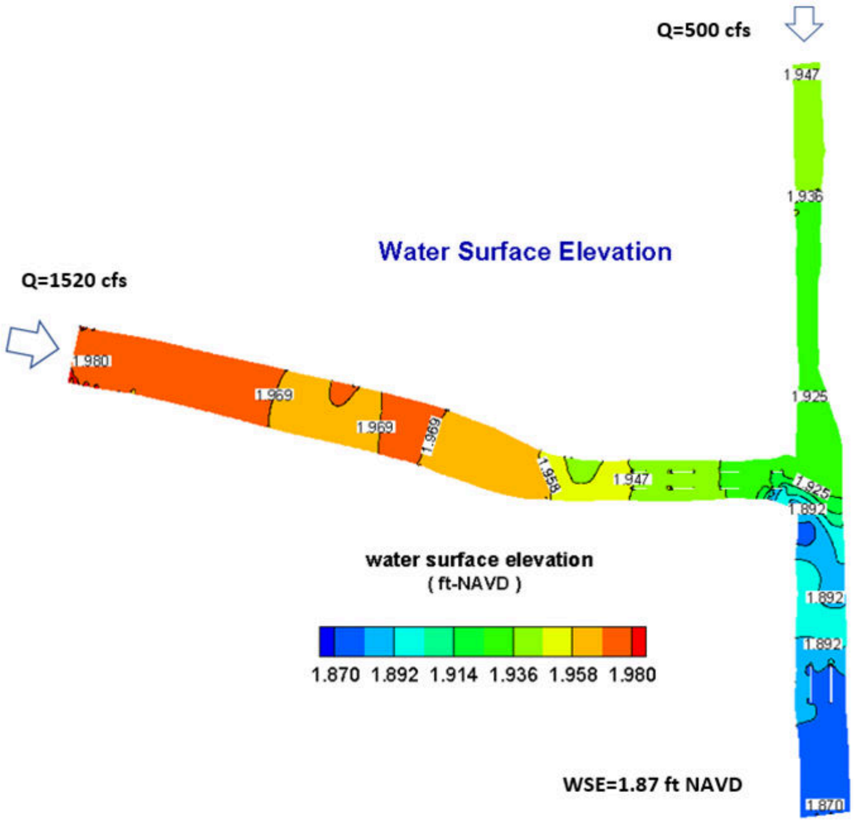

Figure 11. C1N junction free surface elevation based on CFD simulation result, inflow Q1=1520 cfs, Q2=500 cfs, downstream outlet water surface elevation 1.87 ft-NAVD88

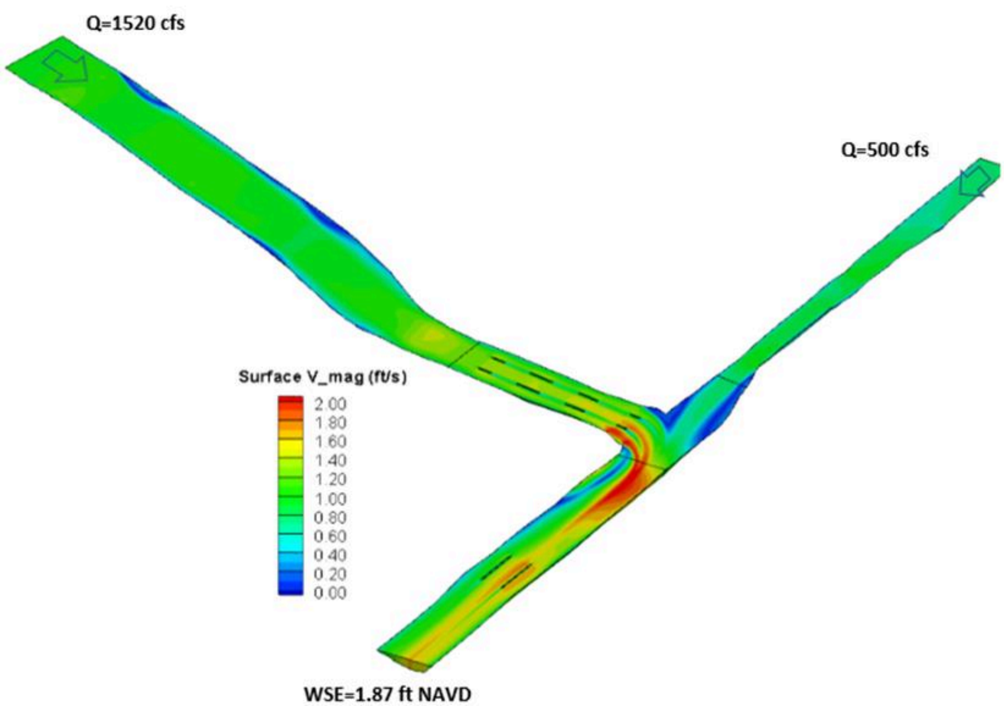

Figure 12. C1N junction free-surface velocity magnitude contours

C1N Junction Simulation Results

The impact of the junction on the flow based on the postprocessed CFD results are shown in Figure 11 to Figure 13. Figure 11 shows the free surface elevations at the C1N junction. The hydrostatic pressure was converted to stage. The junction causes a sudden drop in the energy grade lines of both north and west channels. The figure shows a drop of 0.077 ft. and 0.11 ft. in the water surface at the downstream location compared to the water surface elevations at the north and west inlets. The head-loss induced by the channel junction is quite significant. The 90° change in west channel flow direction, the expansion of the north channel just above the junction, and the zone of flow separation immediately downstream of the junction contributes to the loss in energy.

The streamwise velocity distributions at different locations at the junction, shown in Figure 12, displays that the high flow region starts to change at an area close to the right bank before the junction and gradually shifts towards the left bank after the junction due to the helicoidal motion of the flow. Near the beginning of the junction, the canal bend makes the streamwise velocity distribution asymmetric with higher velocities near the left bank of 2 ft/s. The asymmetricity in velocities near and downstream of the junction can be observed in the velocity magnitude contours at different cross sections near the junction shown in Figure 13.

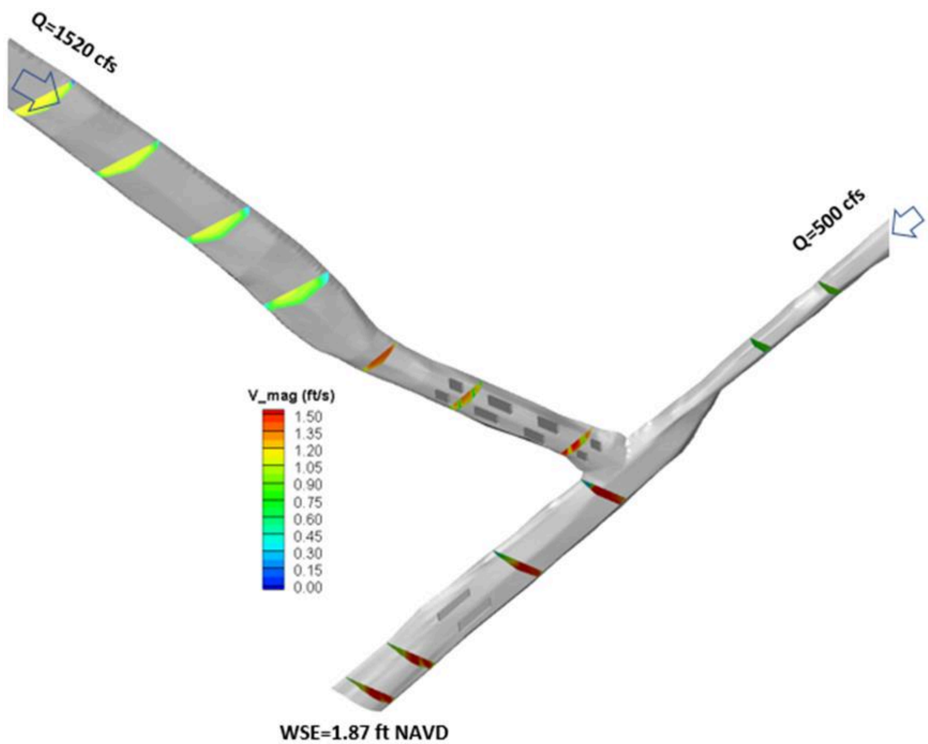

Figure 13. C1N junction cross-section's velocity magnitude contours

CONCLUSION

This study presents a feasible approach to apply CFD and hydrodynamic models to resolve canal capacity problems which require very complicated localized hydraulic loss estimation. The three-dimensional non-hydrostatic CFD model has been successfully applied to investigate the feature of the flow and the associated hydraulic head-loss at the C1 and C1N canal junction located in the C-1 Basin in South Florida. Under the discharge condition of 1520 cfs in the west channel and 500 cfs in the north channel and water stage of 1.87 ft-NAVD at the outlet in the north channel, model results show the C1N channel junction induces a significant drop in the water surface elevations of both north and west channels, and the head loss cannot be ignored for modeling purposes.

The estimated head loss from CFD modeling would be subsequently incorporated into exiting one- and/or two-dimensional hydrodynamic models as a target function to enhance model calibration and optimize the canal conveyance capacity for larger scale hydraulic planning problem in the next phase of the study.

REFERENCE

Best, J. L. and Reid, I. (1984). "Separation zone at open-channel junctions." *J. Hydraul. Eng.*, 110(11), 1588-1594.

Biron, P., Best, J. L., and Roy, A. G. (1996). "Effects of bed discordance on flow dynamics at open channel confluences." *J. Hydraul. Eng.*, 122(12), 676-682.

Ghobadian, R., Tabar, Z. S., and Koochak, P. (2016). "Numerical study of junction-angle effects on flow pattern in a river confluence located in a river bend." *Water SA*, 42(1), 43-51.

Hsu, C. C., Lee, W. J., and Chang, C. H. (1998b). "Subcritical open channel junction flow." *J. Hydraul. Eng.*, 124(8), 847-855.

Hsu, C. C., Wu, F. S., and Lee, W. J. (1998a). "Flow at 90° equal-width open-channel junction." *J. Hydraul. Eng.*, 124(2), 186-191.

Huang, J., Weber, L. J., and Lai, Y. G. (2002). "Three-dimensional numerical study of flows in open-channel junctions." *J. Hydraul. Eng.*, 128(3), 268-280.

Modi, P. N., Ariel, P. D., and Dandekar, M. M. (1981). "Conformal Mapping for channel junction flow." *J. Hydraul. Div., Am. Soc. Civ. Eng*., 107(12), 1713-1733.

Penna, N., De Marchis, M., Canelas, O. B., Napoli, E., Cardoso, A. H., and Gaudio, R. (2018). "Effect of the Junction Angle on Turbulent Flow at a Hydraulic Confluence." *Water*, 10(4), 469.

Ramamurthy, A. S., Carballada, L. B., and Tran, D. M. (1988). "Combining open-channel flow at right-angled junctions." *J. Hydraul. Eng.,* 114(12), 1449-1460.

Shakibainia, A., Tabatabai, M. R. M., and Zarrati, A. R. (2010). "Three-dimensional numerical study of flow structure in channel confluences." *Can. J. Civ. Eng.*, 37(5), 772-781.

Shumate, E. D. (1998). *Experimental description of flow at an open channel junction*. Master's Thesis, Univ. of Iowa, Iowa.

Taylor, E. H. (1944). "Flow characteristics at rectangular open-channel junctions." *Trans. Am. Soc. Civ. Eng*., 109, 893-902.

Weber, L. J., Schumate, E. D., and Mawer, N. (2001). "Experiments on flow at a 90 open-channel junction." *J. Hydraul. Eng.,* 127(5), 340-350.

Weerakoon, S.B. and Tamai, N. (1988) "Three-dimensional calculation of flow in river confluences using boundary fitted co-ordinates." *J. Hydro science and Hydraul. Eng*, 7,51-62.

Wu, R. and Mao, Z. (2003). "Numerical simulation of open-channel flow in 90-degree combining junction." *Tsinghua Science and Technology*, 8(6), 713-718.

Yang, Q. Y., Liu, T. H., Lu, W. Z., and Wang, X. K. (2013). "Numerical simulation of confluence flow in open channel with dynamic meshes techniques." *Adv. Mech. Eng.*, 5, 860431.

Zeng, J., Zhang L. Q., Ansar M., Damisse E., and Castro-Gonzalez, J. A. (2016a). "Applications of computational fluid dynamics to flow ratings at prototype spillways and weirs. I: Data generation and validation." *J. Irrig. Drain. Eng.*, 143(1), 04016072.

Zeng, J., Zhang L. Q., Ansar M., Damisse E., and Castro-Gonzalez, J. A. (2016b). "Applications of computational fluid dynamics to flow ratings at prototype spillways and weirs. II: Framework for planning, data assessment, and flow rating." *J. Irrig. Drain. Eng.*, 143(1), 04016073.

Zeng, J., Ansar, M., Raymond, J., Rakib, Z., and Zhang, L. (2018a). "Automated water control structures flow rating using CFD generated data." *Proc., World Environmental and Water Resources Congress*, ASCE, Minneapolis, Minnesota, 188-196.

Zeng, J., Rakib, Z., and Bobsein, J. (2018) *Application of Computational Fluid Dynamic Model for C1N Canal T-Junction Water Head Loss Study*. Technical Memo, Applied Hydraulics Section, South Florida Water Management District, October 2018.

Zeng, J., Rakib, Z., Ansar, M., Dessalegne, T., and Hajimirzaie, S. (2018b). "Applications of CFD for flow rating at complex water control structures." *Proc., World Environmental and Water Resources Congress*, ASCE, Minneapolis, Minnesota, 210-221.

Assessment of Reservoir Sedimentation and Mitigation Measures: A Case Study of Palo Redondo Reservoir

Katherine Velásquez-Castro[1]; Eusebio Ingol-Blanco[2]; Richard Pehovaz-Alvarez[3]; and Carlos Cruzado-Blanco[4]

[1]Civil Engineering, Pontifical Catholic Univ. of Peru, Lima 32. E-mail: velasquez.kb@pucp.pe
[2]Pontifical Catholic Univ. of Peru; National Agrarian Univ.-La Molina; Peruvian Univ. of Applied Sciences, Lima 32. E-mail: eingol@pucp.edu.pe
[3]Pontifical Catholic Univ. of Peru, Lima 32. E-mail: pehovaz.rp@pucp.pe
[4]San Pedro Univ., Lima 11. E-mail: carlos.cruzado@usanpedro.edu.pe

ABSTRACT

The accelerated sedimentation of the main Peruvian reservoirs has caused losses of the useful storage capacity that significantly affects the water allocation to the different users. This research aims to evaluate the sedimentation risk of Palo Redondo Reservoir of the Chavimochic hydraulic system, located in La Libertad region of Peru's northern, proposing alternatives to reduce its impacts. The reservoir was designed for a total capacity of 400 MCM, however, it is likely that in the future it has an accelerated sedimentation problem due to the high erosion of the Santa River Basin and because of its water uptake system whose sand trap has an efficiency less than 75%. The methodology includes the modeling for the prediction of stream flow and sediment yield in the Tablachaca sub-basin which is a critical drainage area of the Santa River Basin, using the soil and water assessment tool (SWAT). Likewise, it includes the modeling of sediment yield in the Palo Redondo small sub-basin using the kinematic runoff and erosion model (KINEROS). It could be activated during the occurrence of the El Niño phenomenon causing maximum discharges with high rates of sediment transport to the reservoir. The SWAT calibration results show a good model performance with NASH coefficients greater than 0.6 for flow rates and sediment concentrations, respectively. On the other hand, the land cover change in Tablachaca sub-basin shows a significant reduction in erosion rates and, therefore, a significant reduction of sediments towards the Palo Redondo Reservoir.

Key words: Sedimentation, Palo Redondo reservoir, SWAT modeling, Santa River.

INTRODUCTION

The largest dams in Peru have been affected by a more accelerated sedimentation than estimated in their designs. The references of premature collapse, as consequence of the high potential of soil erosion of the Pacific basins, suggest not to build large dams in basins under these hydrological characteristics (Rocha 2006; Ortiz et al. 2015). Unless rigorous basin management and sediment control programs are implemented; preferably a little earlier or at least at the same time as the physical execution of the project.

Therefore, the construction of the Palo Redondo Dam, part of the third stage of the Chavimochic project, which captures waters from the Santa River basin, located on the Pacific Coast, has been the subject of huge discussion in the last decades. Rocha (1999) indicates that the amount of sediment estimated to reach Palo Redondo would be very high due to the large production of the basin and the deficient Chavimochic sand trap.

Given this, it arises as a question, whether the performance of the future Palo Redondo Dam will be adequate or will suffer a premature collapse due to excessive sedimentation as occurs with dams of similar characteristics. Specifically, ¿What will be the sediment rates that will enter the Chavimochic system? ¿What structural measures can be implemented to reduce the amount of sediment that reaches the reservoir? ¿What are the methods of watershed management and in what areas of the Santa river basin should they be applied to decrease the rate of sediment production in the basin?. Therefore, this research aims to evaluate the sedimentation risk of Palo Redondo reservoir of the Chavimochic hydraulic system, located in La Libertad region of Peru's northern (Figure 1), proposing alternatives to reduce its impacts. Figure 1 shows the location of the study area, including the main hydraulic infrastructure of the Chavimochic Project (Intake, Sand trap, Dam); as well as the control stations that will feed the dam where we can estimate the amount of sediment that will accumulate in the Palo Redondo Reservoir.

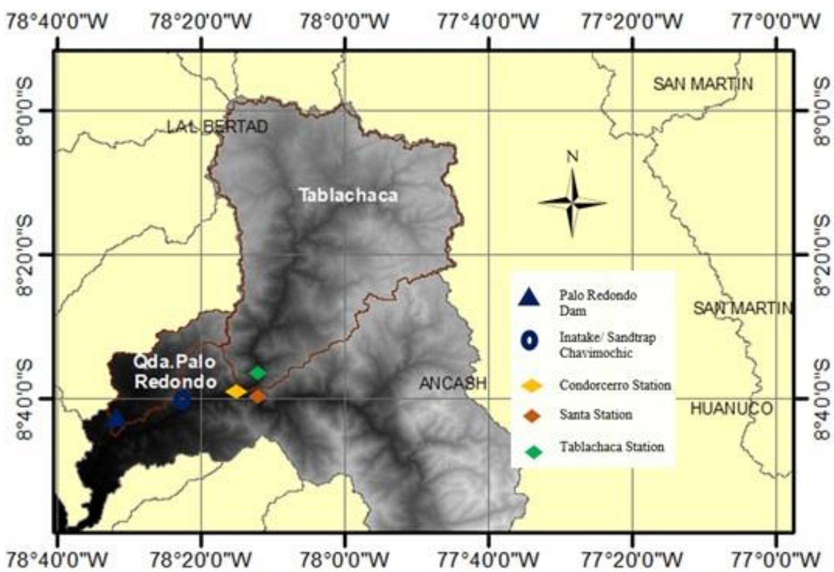

Figure 1. Location of study area

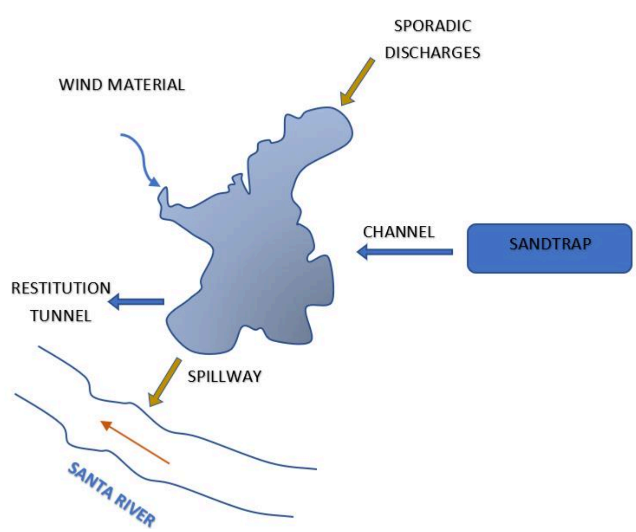

Figure 2. The Palo Redondo Dam System (PECH, 2013)

METHODOLOGY

Assess the potential causes and consequences of sedimentation of the future Palo Redondo reservoir

The state of the two largest dams in Peru was studied, with problems of accelerated sedimentation: Poechos and Gallito Ciego. This allowed identifying the risks to which the Palo Redondo Dam is exposed. Likewise, the analysis of the Palo Redondo Dam System allowed identifying the origin of the solids that will be deposited in the reservoir. Figure 2 shows the solids that will enter to the reservoir come from the feeding channel, the sporadic discharges from the Palo Redondo Stream and the wind material. In this research, the sediment production was analyzed taking account the first two causes previously mentioned because of they are the ones with the greatest impact.

Assess the sediment production in the Palo Redondo sub-basin under extreme events proposing structural control measures

The study of the Palo Redondo sub-basin allowed to characterize it as a dry sub basin with scarce rainfall, but with probability of extraordinary events with serious consequences such as those caused by the El Niño Phenomenon (1983, 1998 and 2017). Therefore, the probable maximum precipitation was analyzed, as well as the resulting liquid and solid hydrograph considering a Type II rainfall distribution, by means of the Kineros model. For the delimitation and descretization of the sub-basin in Kineros Model, the Palo Redondo DEM (Digital Elevation Model) obtained from the MINAM Geoserver was required. It has a spatial resolution of 30 meters and it was projected in the 17S zone.

The model parametrization was done using the FAO soil type maps, as well as the map of use and land coverage obtained from the MINAM (2015), which was reclassified for its interpretation in Kineros under the NALC category.

Assess sediment production in critical areas of the Santa River Basin

In order to determine the areas with the greatest sediment contribution, it was necessary to analyze the Condorcerro station and two stations upstream: Tablachaca and Santa. Studies carried out by Morera (2011) and the PECH (2010), had previously determined the water and solid contribution of the mentioned stations between 2000 and 2010. It was concluded that the Tablachaca sub-basin contributes about 57.7% of the total suspend solids of the Santa River Basin (Morera, 2011).

Consequently, it was decided to analyze the sediment production in the Tablachaca sub-basin using SWAT as modeling tool. The configuration of the model, projected in the 18S zone, required a DEM, vegetation coverage map and soil type map for the Tablachaca sub-basin. It included the rainfall analysis of the stations available in the study area. In this regard, it was found that historical rainfall data were very scarce, which is why we worked with data from the PISCO tool (Peruvian Interpolate data of the SENAMHI's Climatological and Hydrological Observations), which combines data observed of weather stations and remote sensing data. It includes records of precipitation since 1981.

Likewise, the model calibration is developed thanks to the flow and sediment concentrations records of the PECH (Proyecto Especial Chavimoch) for the Condocerro y Tablachaca stations. Calibrating the model involved both quantitative and qualitative evaluation of the hydrologic response of each subcatchment (Ingol and Mckinney 2013). This was carried out by comparing monthly observed and simulated streamflow at the outlet of the subcatchment, as well the monthly observed and simulated concentrations. The SWAT calibration results show a good model performance with NASH coefficients greater than 0.6 for flow rates and sediment concentrations, respectively. In addition, five alternative scenarios were proposed to the current land coverage of the sub-basin, which were also analyzed using the SWAT model in order to compare changes in solid and liquid flows. The first scenario reflects the current situation of the Tablachaca basin based on the vegetation map of the MINAM in 2013. The second scenario reflects an ecological improvement in the areas with Andean pajonal and shrubland bog, changing its status from poor to medium. The third scenario improves the conditions of the previous scenario to show the results of a high ecological status. The fourth scenario increases forest plantation in desert areas with insufficient vegetation cover. The fifth scenario takes into account all the previous improvements, increasing the forest plantation by up to 20%, compared to the first scenario, considering its development in the areas of greatest erosion danger in the basin.

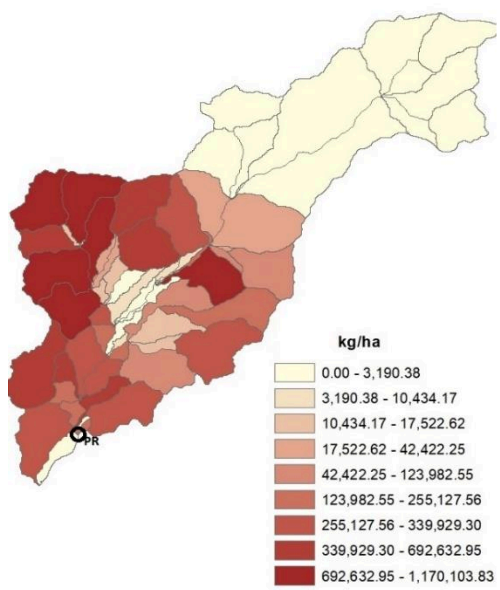

Figure 3. Erosion map of the Palo Redondo sub-basin

RESULTS

Erosion map of the Palo Redondo sub-basin

Figure 3 shows the erosion of the Palo Redondo sub-basin that would cause a storm type SCS II, simulated by Kineros model, being able to identify that the area's most prone to erosion are the closest to the area of the reservoir.

Volume of suspended sediments caused by storm

Table 1 shows results of the simulation for the total sediment rate and according to each particle size. In addition, the average specific weight of the sediment load, the total sediment load and the total volume of sediment were estimated. To estimate the sediment load, it was considered that the PMP would only produce precipitation in 80% of the basin as suggested by PECH (1990). The results indicate an average specific weight of 1.17 Ton / m^3, which suggests a torrential flow (Costa 1988). In order not to overestimate or underestimate the results as well as considering that the Type II curve represents storms in Peruvian Coast, only the volume obtained by the Type II hietogram was considered; likewise, it was valued that only 2 storms of such intensity would occur during the reservoir lifetime. As result, it has been estimated a total of 6.62 MCM of sediments that would reach the reservoir due to two storms in the Palo Redondo sub basin.

Table 1. Volume of sediments caused by storm

Sediment	Rain Type II		
	Rate of sed. (Ton/ha)	Sed. (%)	ϒ (Ton/m^3)
Sand	25.26	20	0.30
Silt	77.03	62	0.74
Clay	22.17	18	0.13
Total	124.46	100	1.17
Ton			3,883,255
1 tormenta (MCM)			3.31
2 tormentas (MCM)			6.62
3 tormentas (MCM)			9.93

Erosion map of the Tablachaca sub-basin

Figure 4 shows the erosion of the Tablachaca sub basin, being able to identify the high rates of erosion in each sub-basin that lead to the average rate of 364 Ton / ha.

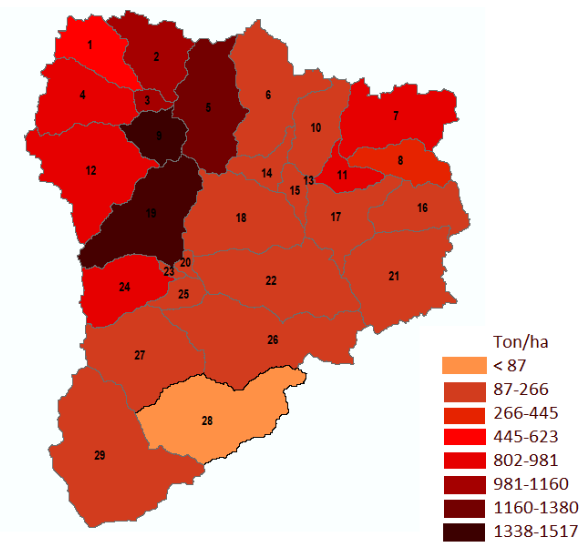

Figure 4. Erosion map of the Tablachaca sub-basin

Erosion rate of each scenario

The results in Table 2 shows a low decrease in sediment production between Scenarios 3 and